Journal of Alloys and Compounds 622 (2015) 1–7

Contents lists available at ScienceDirect

Journal of Alloys and Compounds

journal homepage: www.elsevier.com/locate/jalcom

Synthesis and characterization of Ho^{3+}-doped strontium titanate downconversion nanocrystals and its application in dye-sensitized solar cells

Y.Y. Li [a,b], H.S. Hao [a,b,*], L. Qin [c], H.L. Wang [a,b], M.Q. Nie [a,b], Z.Q. Hu [a,b], W.Y. Gao [a,b], G.S. Liu [a,b]

[a] Department of Inorganic Nonmetallic Materials Engineering, Dalian Polytechnic University, Dalian 116034, China
[b] Liaoning Provincial College Key Laboratory of New Materials and Material Modification, Dalian Polytechnic University, Dalian 116034, China
[c] National Engineering Research Center of Seafood, Dalian Polytechnic University, Dalian 116034, China

ARTICLE INFO

Article history:
Received 19 August 2014
Received in revised form 30 September 2014
Accepted 30 September 2014
Available online 13 October 2014

Keywords:
Ho^{3+}-doped strontium titanate
Downconversion
Dye-sensitized solar cells
Photoluminescence

ABSTRACT

Ho^{3+}-doped strontium titanate ($SrTiO_3$:Ho^{3+}) downconversion (DC) nanocrystals are synthesized by the solid state interaction of titanium dioxide, strontium nitrate, holmium oxide and sodium chloride and then used as a photoanode in dye-sensitized solar cells (DSSCs) to investigate the effect of DC nanocrystals in DSSCs. Differential thermal analysis, X-ray diffraction, scanning electronic microscope, energy dispersive spectroscopy and Brunauer–Emmet–Teller analysis confirmed the formation of cubic structured $SrTiO_3$:Ho^{3+} nanocrystals with diameters of 40–400 nm, pore size of ~45 nm, sintering temperature of 950 °C. The photofluorescence and UV–Vis absorption spectra of the $SrTiO_3$:Ho^{3+} nanocrystals revealed strong emission intensity and visible light absorption when doped content of holmium oxide was between 1 wt% and 3 wt%. Compared with the pure $SrTiO_3$ photoanode, $SrTiO_3$:Ho^{3+} DC photoanode showed a greater photovoltaic efficiency. The photoelectric conversion efficiency (η) of the DSSCs with a $SrTiO_3$:Ho^{3+} photoanode doped with 1 wt% holmium oxide was 59% higher than that with a pure $SrTiO_3$ photoanode. This phenomenon could be explained by $SrTiO_3$:Ho^{3+} nanocrystals' ability to absorb ultraviolet light and downconvert it to visible light, which extends spectral response range of DSSC to the ultraviolet region and increased the short-circuit current density (Jsc) of DSSCs.

1. Introduction

Solar energy has been considered as a green and renewable alternative energy source to traditional fossil fuels [1]. Since the prototype of a DSSC was reported in 1991 by O'Regan and Gratzel [2], it has aroused intensive interest and become one of hotspots in solar energy field, because of its ease of fabrication and cost-effectiveness compared with silicon-based photovoltaic devices [3,4]. However, it has been believed that ultraviolet light can degrade the organic dyes in DSSCs in the long term [5]. In addition, the quantum efficiency of DSSCs in the ultraviolet wavelength range is relatively lower than in the visible light wavelength range [6]. Thus, it is desirable to downconvert the ultraviolet light into visible light within the photoanodes of DSSCs. The most effective route for downconverting the ultraviolet light into visible light is doping rare-earth compounds.

Rare-earth ions are +3 value cations. When they are doped into semi-conductor, a p-type doping effect occurs [7,8], which results in the elevation of Fermi level of the photoanode, and turns to the enhancement of the photovoltage of the DSSCs. The introduction of doped rare-earth compound not only increases the photocurrent via conversion luminescence, but also improves the photovoltage by p-type doping effect. This double function is very significant for enhancing the photovoltaic performance of the DSSCs. Unfortunately, little significant research on conversion luminescence and/or p-type doping effect by rare-earth ions in the DSSCs has been attempted [9–11]. Until now, as the highest magnetic moments among the rare earth metal ions, holmium (III) has been used widely as a magnetic material [12]. Moreover, Lewis acid sites and highly reactive base sites (O^{2-} and/or OH^-) were scattered on the surface of holmium oxide (Ho_2O_3) [13]. The photoelectric performance of $SrTiO_3$ can be improved through OH^- reacting with holes and obtained hydroxyl radical. Otherwise, as the earliest multivariate oxide had been studied in DSSC, the band gap of $SrTiO_3$ is 3.2 eV, which has structural similarity with TiO_2. As has been reported [14], Burnside's team prepared $SrTiO_3$ particles by hydrothermal method and acquired the efficiency of

---

* Corresponding author at: Department of Inorganic Nonmetallic Materials Engineering, Dalian Polytechnic University, Dalian 116034, China. Tel.: +86 41186323708; fax: +86 41186323438.

E-mail address: beike1952@163.com (H.S. Hao).

http://dx.doi.org/10.1016/j.jallcom.2014.09.223
0925-8388/

1.8%. Furthermore, the investigation on holmium doping in $SrTiO_3$ has rarely been reported.

For elements doped $SrTiO_3$, the change in electronic band structures can be divided into two kinds: (1) forming a new mid gap state between the valence band (VB) and conduction band (CB), such as Rh, Cr, Ir, or Ru doped $SrTiO_3$ [15–18]. (2) Changing the VB or CB through the mixing of energy level between dopant and host elements, such as N, F, C, or S doped $SrTiO_3$ [19–23].

In this research paper, $SrTiO_3$:Ho^{3+} nanocrystals are synthesized by the solid state method and the Ho^{3+} doped content that crucially affect the optical properties of the synthesized nanocrystals were optimized. Besides the morphology, crystal structure and pore characteristics of the samples were investigated. Finally, the effect of produced nanostructures as DC photoanode in DSSCs was investigated.

2. Experimental

2.1. Synthesis of $SrTiO_3$:Ho^{3+} nanocrystals

$SrTiO_3$ doped with 0 wt%, 0.5 wt%, 1 wt%, 3 wt%, 5 wt%, 8 wt% holmium oxide ($SrTiO_3$:Ho^{3+}) nanocrystals were labeled as S0, S1, S2, S3, S4, S5 in sequence and synthesized by the solid state method. Appropriate amounts of titanium dioxide (TiO_2, Degussa P25), strontium nitrate ($Sr(NO_3)_2$), holmium oxide (Ho_2O_3) and sodium chloride (NaCl) were mixed and heated in an alumina crucible at 950 °C for 24 h after milling, and then cooled to room temperature. All the heat treatments were carried out under air atmosphere. The obtained powders were washed with deionized water to remove NaCl. The resulting samples were finally dehydrated by heating at 120 °C for 24 h. Thus, $SrTiO_3$:Ho^{3+} nanocrystals were obtained.

2.2. Fabrication of DSSCs based on $SrTiO_3$:Ho^{3+} nanocrystal photoanode

Fluorinated tin oxide (FTO) glass sub-strates were cleaned with sodium hydroxide solution, deionized water and ethanol for 30 min before use. The TiO_2 blocking layer for DSSCs was prepared according to following strategy: tetrabutyl titanate was mixed with diethanolamine and absolute ethyl alcohol, and the mixture was stirred for 5 min. Then appropriate deionized water was added dropwise, and the mixture was stirred continued for another 30 min until the solution became colloidal sol for the coating preparation. The obtained colloidal sol was coated on FTO by spin-coating method. The film was then sintered at 500 °C for 30 min. In the next step, mesoporous $SrTiO_3$:Ho^{3+} film was deposited onto surface of TiO_2 blocking layer by screen printing method. Appropriate $SrTiO_3$:Ho^{3+} powder was added into the agate mortar and mixed with moderate deionized water and acetic acid. After grinding for about 5 min several drops of triton X-100 were added and then the mixture was grinded for another 1 h until the slurry became viscous enough to screen print the porous membrane. The mesh number of the screen is 200 meshes. The films were dried under ambient conditions and then annealed at 500 °C for 30 min to remove the binders in the paste. Then, the films were cooled down to 80 °C for dye sensitization. Dye sensitization was achieved by immersing the $SrTiO_3$:Ho^{3+} electrodes in a 0.5 mM N719 dye in ethanol solution overnight at room temperature in the dark. After being removed from the dye solution, the electrodes were rinsed and dried. Finally, unsealed sandwich type solar cells, assembled with dye sensitized $SrTiO_3$:Ho^{3+} (S0–S5) electrode as photoanode, Pt coated FTO electrode as the counter electrode, and standard iodide electrolyte solution as a mediator, were labeled as W0–W5 in sequence. The area of $SrTiO_3$:Ho^{3+} working electrode was 0.25 cm^2 and the thickness of the film electrode was kept almost the same.

For comparison, non N719 sensitized c-W0 and d-W2 $SrTiO_3$:Ho^{3+} film electrode were made, and then the e-W0 and f-W2 film electrode without blocking layer were also fabricated. Here, it should be mentioned that all the experimental conditions were kept identical to avoid experimental errors.

2.3. Characterization

The volatilization temperatures of the organic phases and the transformation of the inorganic phases were investigated by differential thermal analysis (DTA, WCR-2D). The phase and crystallinity of samples were analyzed by X-ray diffraction (XRD, D/max 3B) using Cu Kα radiation (40 kV, 60 mA). The surface morphology and composition were examined by scanning electron microscope (SEM, JSM-6460LV) equipped with the energy dispersive spectroscopy (EDS, X-Max50). The pore characteristics of the as prepared powder were investigated by Brunauer–Emmett–Teller (BET) method using nitrogen adsorption–desorption analyzer (SSA-4200, Bulder, Beijing). The optical properties were measured by UV–Vis absorbance spectrometer (UV–Vis, Lambda35). The photoluminescence (PL) spectra were analyzed by fluorescence spectrometer (LS-55). A solar simulator (SSA50) providing an illumination of AM1.5G simulated sunlight with 100 mW/cm^2 irradiation and a Keithley 2400 source meter were employed to measure the photovoltaic properties of the assembled DSSCs. The monochromatic incident photon–electron conversion efficiency (IPCE) of DSSCs was also measured by light meter (SM-25, Japan).

3. Results and discussion

3.1. DTA analysis

Fig. 1 shows the DTA curves of S0 and S2 with Ho_2O_3 of 0 and 1 wt% in air atmosphere. Both curves showed four events. As for S0, the first endothermic event between 420 and 487 °C (T peak = 462 °C), the second event between 589 and 688 °C (T peak = 646 °C), the third event between 759 and 796 °C (T peak = 786 °C) and the fourth event between 831 and 1187 °C (T peak = 1123 °C) correspond to the stripping of crystalline water, the decomposition of Sr $(NO_3)_2$, the melting of NaCl and the formation of $SrTiO_3$, respectively. As for S2, all peaks have a slightly move to left. This may be related to Ho^{3+} ions which may impact the crystal form of $SrTiO_3$. Based on the DTA results, the temperature necessary for the starting form of the $SrTiO_3$ is almost 900 °C. Thus, the samples were sintered at 950 °C.

3.2. XRD patterns of $SrTiO_3$:Ho^{3+}

As shown in Fig. 2, the XRD patterns of S0, S2 and S5 doped with Ho_2O_3 of 0, 1 wt% and 8 wt% in sequence. All diffraction peaks of the prepared samples are readily indexed as cubic phase of $SrTiO_3$ and consistent with the standard pattern (PDF#35-0734). This indicates the formation of the cubic phase of $SrTiO_3$. Bragg's reflections from $SrTiO_3$ nanocrystals were observed in XRD patterns at 2θ values of 23°, 32°, 40°, 46°, 58° and 68° representing (100), (110), (111), (200), (211) and (220) planes of cubic phase and space group of Pm3m with the lattice constants of $a = b = c =$ 0.3905 nm. Although the diffraction peaks of these samples were in the similar position, slight shift of the peaks could be observed when the content of Ho_2O_3 reached 8 wt% (S5). For Ho^{3+} ion, due to its smaller size than Sr^{3+} ion (Ho^{3+}: 0.901 Å, Sr^{3+}: 1.18 Å), distortions could be found in the doped $SrTiO_3$ lattice network. According to the Bragg equation ($2d\sin\theta = n\lambda$), when smaller Ho^{3+} ions substituted for Sr^{3+} ion, lattice distortions led to the decrease of interplanar distance. Thus, the corresponded diffraction peaks shifted to the larger-angle direction. Besides, as the amount of doping ions increased, the shifting degree increased. The crystal distortions also provided evidence that Ho^{3+} ions were introduced into the

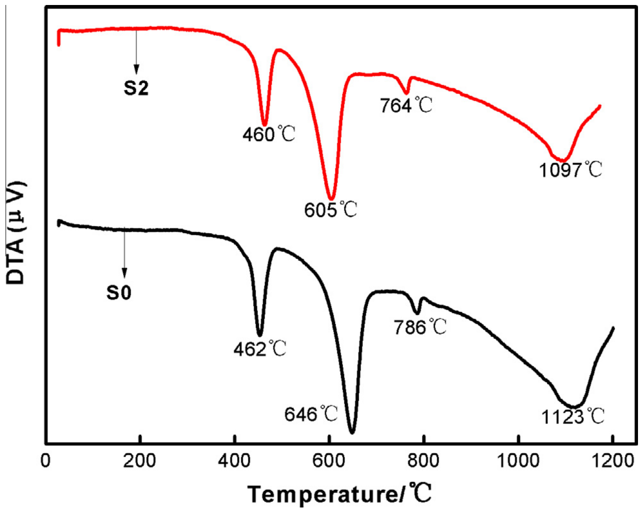

Fig. 1. DTA curves of S0 and S2 with Ho_2O_3 of 0 and 1 wt% in air atmosphere.